Publication P2

A. Tarkiainen, M. Liljeström, M. Seppä, and R. Salmelin. 2003. The 3D topography of MEG source localization accuracy: effects of conductor model and noise. Clinical Neurophysiology, volume 114, number 10, pages 1977-1992.

ELSEVIER

Clinical Neurophysiology 114 (2003) 1977–1992

www.elsevier.com/locate/clinph

The 3D topography of MEG source localization accuracy: effects of conductor model and noise

A. Tarkiainen*, M. Liljeström, M. Seppä, R. Salmelin

Brain Research Unit, Low Temperature Laboratory, Helsinki University of Technology, P.O. Box 2200, 02015 HUT, Espoo, Finland

Accepted 1 June 2003

Abstract

Objective: To evaluate the effect that different head conductor models have on the source estimation accuracy of magnetoencephalography (MEG) under realistic conditions.

Methods: Magnetic fields evoked by current dipoles were simulated using a highly refined 3-layer realistically shaped conductor model. Noise from a real MEG measurement was added to the simulated fields. Source parameters (location, strength, orientation) were estimated from the noisy signals using 3 spherically symmetric models and several one- and 3-layer realistically shaped boundary-element models. The effect of different measurement sensors (gradiometers, magnetometers) was also tested.

Results: The noise typically present in brain signals masked the errors due to the different conductor models so that in most situations the models gave comparable results. Active cortical areas around the vertex and in the temporal, frontoparietal, and occipital regions were typically found with 2–4 mm accuracy, whereas source localization in several anterior frontal lobe and deep brain structures yielded errors exceeding 2 cm. Localization in anterior frontal regions may benefit most from the use of realistically shaped models.

Conclusions: The traditionally used sphere model is an adequate model for most research purposes. Any means that increase the signal-to-noise ratio are of highest importance in attempting to improve the source estimation accuracy.

Keywords: Magnetoencephalography; Current dipole; Simulation; Source estimation; Sphere model; BEM

1. Introduction

From the measured magnetoencephalographic (MEG) or electroencephalographic (EEG) signals, it is possible to estimate the underlying neural activity and localize it to a certain part of the brain. The accuracy of this procedure depends on many factors such as the true location, shape, and extent of the neural currents that generated the measured signal, the environmental noise present in the measurement, the interfering activation from other brain areas, the accuracy of the conductor model used to describe the conductivity geometry of the head, the accuracy of the head position measurement that indicates the location of the head with respect to the measurement device, the possible head movements during the measurement (in MEG), and the accuracy of combining functional information with anatomical information. Despite the large number of variables affecting the results, experience has shown that under good conditions, active brain areas can be localized accurately and reliably with MEG (Rose et al., 1991; Godey et al., 2001; Mäkelä et al., 2001).

A common, efficient, and physiologically meaningful approach to identify active brain areas is to assume that at a given time, and in a certain region, there is only one active source area, which can be represented by a current dipole. This assumption simplifies the mathematics dramatically and the dipole location, orientation, and amplitude, representing the center of the active area and the direction and amount of current flow therein, can be determined directly from the distribution of the MEG signal values with a least-squares search. Accordingly, the single dipole model is still the most widely used method. During the past few years, many new techniques, such as the minimum current estimate (Uutela et al., 1999), RAP-MUSIC (Mosher and Leahy, 1999), anatomically and physiologically constrained statistical parametric mapping (Dale et al., 2000), and beamformer techniques (see e.g. Sekihara et al., 2001;

* Corresponding author. Tel.: +358-9-4516159; fax: +358-9-4512969.
E-mail address: antti.tarkiainen@hut.fi (A. Tarkiainen).

1388-2457/03/$30.00
doi:10.1016/S1388-2457(03)00195-0

Gross et al., 2001) have offered new possibilities for the source localization problem in MEG. The success of all these source localization approaches, however, depends on the factors listed above. Two of these factors are of particular importance, namely, the signal-to-noise ratio of the measured signals and the conductor model used to describe the conductivity geometry of the head.

All real measurement signals contain noise. The signal-to-noise ratio of the measured data is affected by the measurement hardware, shielding against external noise sources, signal-processing techniques, selection of the studied brain area, and the paradigm and stimuli used in the measurement. The conductor model, on the other hand, is a mathematical construction that is built to approximate the true conductivity geometry of the head. The simplest and most popular model is the spherically symmetric model where the brain volume is approximated by a sphere. Realistically shaped one-layer boundary-element models take into account the true shape of the brain and 3-layer models also that of the skull and the scalp. Local conductivity differences and even the anisotropy of the head can be accounted for by using finite-element models. These refined models offer a more realistic description of the shape and conductivities of the head, but at the expense of heavily increased computing time.

Even though computers nowadays make the use of realistically shaped head conductor models more feasible than ever before, the spherically symmetric model is still the most popular one in everyday research. The main reasons for this are the ease of creating the model, the fast calculations, and the familiar and well-known behavior of the model, together with the fact that a sphere is—for the most part—a quite reasonable approximation for the human head. The use of realistically shaped boundary-element models is also relatively widespread and, at present, they offer a potential alternative for the spherical models. The selection of the conductor model is an important practical question that has to be answered every time when a researcher starts to analyze a new set of data. Therefore, it is important to know the impact of different head models on the localization accuracy of MEG in order to decide when more sophisticated models should be used and when it is adequate to use the simple spherical head model.

The properties and bias induced by the use of different kinds of conductor models have been studied mainly in 3 ways. The most realistic measurement situation can be achieved by utilizing implanted brain electrodes as current sources (see e.g. Balish et al., 1991; Rose et al., 1991; Cuffin, 1996). However, this method is understandably limited as the number and configuration of the electrodes are very restricted. Electrodes can be distributed more freely in a phantom that is built to mimic the structure of a real head (see e.g. Menninghaus et al., 1994; Leahy et al., 1998) but even with phantoms, the number of electrodes must be relatively small and one cannot vary the source orientations freely. In addition, the measurement situation is not as realistic as with a real subject, because only background magnetic noise from the environment and measurement hardware is present and, if desired, the interfering brain activation has to be taken into account otherwise. With computer simulations, the current sources can be configured freely and a large number of possible situations can be studied. The most problematic feature with simulations is the selection of the reference model because the results will describe the differences between the reference model and the models used in the source localization. To get information about how brain models will work with real MEG/EEG data, one has to use a reference model that mimics the real situation as closely as possible. Unfortunately, the complexity of the model is often restricted by computational resources. Also, if wanted, the effect of noise has to be added to the simulated fields as realistically as possible. So far, simulation studies have mainly concentrated on the intrinsic differences between conductor models and they have thus been carried out without any noise (Yvert et al., 1997; Fuchs et al., 1998a, 2001; Crouzeix et al., 1999). However, noise is present in every real data set and, therefore, it is essential to know the impact it has on the performance of different conductor models.

In the present study, we used computer simulations to mimic real MEG data with real noise to study the localization accuracy of MEG. This work was performed using the single dipole model due to its simplicity, wide use, and ease of quantifying the associated errors. Specifically, we evaluated: (i) the typical magnitude of localization, orientation, and amplitude errors related to using spherical conductor models, one-layer realistically shaped boundary-element conductor models, and 3-layer realistically shaped boundary-element conductor models in analyzing the neural activity generated in different parts of the brain and (ii) the relative performance of these models under realistic conditions. The main goal of the study was to find out whether it is adequate to use the simple and fast spherical head model in MEG source estimation or whether the realistically shaped boundary-element models offer such an advantage that their use is justified or even recommended. In addition to the comparison of head conductor models, we compared the effect that different MEG sensor types (first-order planar gradiometers and magnetometers) as well as the correctness of the conductivity value of the skull have on the source estimation errors.

2. Methods

2.1. Magnetoencephalography

MEG detects the weak magnetic fields created by synchronous activation of thousands of nerve cells. This noninvasive measurement is conducted outside the head using extremely sensitive superconducting quantum interference device (SQUID) sensors. From the distribution of

the measured magnetic fields, the parameters of the underlying cortical activation can be estimated. Often, the active source areas are modeled as equivalent current dipoles. This approach is based on the assumption that the activated cortical area is small and can, therefore, be modeled using a point-like current dipole with certain location, orientation, and strength. For a comprehensive review of MEG and related mathematics, see Hämäläinen et al. (1993).

In the present study, the simulations were generated using the sensor configuration of a 306-channel Vectorview™ magnetometer (Neuromag Ltd, Helsinki, Finland). Vectorview™ employs a helmet-shaped array of SQUID sensors, which covers most of the cortical surface. In this array, there are 102 different sensor locations. At each location, there are 3 sensors: two orthogonal first-order planar gradiometers (204 gradiometers in total) and one magnetometer (102 magnetometers in total). Planar gradiometers are most sensitive to neural currents right underneath the sensor, while magnetometers can detect activation generated in deep brain structures better but they are also more sensitive to distant noise sources.

2.2. Simulations: the basic concept

The purpose of the present study was to investigate the 3D topography of MEG source estimation accuracy under different, but realistic conditions. To imitate a real measurement situation, we added noise collected in a real MEG recording to the simulated magnetic fields. Our first goal was to evaluate how estimation errors depend on the studied brain region. To do this, we studied a dense grid of possible source locations distributed evenly throughout the whole brain and classified the results according to the area and source depth. To investigate the effect of the conductor model on source estimation, this operation was repeated with 13 different conductor models, including spherically symmetric models, one-layer realistically shaped boundary-element models, and 3-layer realistically shaped boundary-element models. To study how estimation errors depend on the signal-to-noise ratio of the MEG signals, the source localization was carried out while varying the frequency band of the noise and the original source strengths. Furthermore, we tested how the sensor type used to collect the signals affects the accuracy of source estimation by calculating the localization errors using data measured by planar gradiometers only, magnetometers only, or a combination of both. This part of the study was done with only 3 representative conductor models: one spherical, one one-layer realistically shaped, and one 3-layer realistically shaped model, selected on the basis of the results of the conductor model comparison.

The first step in the simulations was to select as accurate a reference model as possible. This model was then used to compute the magnetic fields generated by the simulated sources. The magnetic fields were calculated as seen by the 306-channel Vectorview™ neuromagnetometer, which has the advantage that it incorporates both magnetometers and gradiometers at the same locations. Noise was taken from real MEG data measured using the same neuromagnetometer. Source parameters (location, amplitude, and orientation of equivalent current dipoles) were then estimated from the magnetic fields using the different head conductor models and applying techniques that are typical also in real data analysis. To get reliable results, the procedure was repeated 9 times at each studied source location and the estimation errors for that location were calculated as an average of the repetitions. These repetitions differed both in the orientation of the original simulated dipole source and the exact noise pattern that was taken from the real MEG data set and added to the simulated fields. All these procedures are described in detail in the following sections.

2.3. Conductor models

Different tissues and substances have different conductivities, which affects the flow of electric current and the propagation of electro-magnetic fields. In order to calculate the simulated magnetic fields or find the sources that can explain measured magnetic fields, one has to approximate the conductivity geometry of the head with some model.

The mathematically simple, computationally efficient, and easily formed spherical model approximates the shape of the brain with a sphere. Spherical models are typically created with the help of the subject's magnetic resonance images (MRIs); the origin of the sphere is selected so that the shape of the sphere fits best the local curvature of the main brain areas of interest, e.g. occipital and parietal lobes or frontal lobe. In the present study, we used 3 different spherical models in source localization. BRAINSPH was fitted to match the curvature of the reference brain model, i.e. it was fitted to match the shape of the whole brain as well as possible and not to favor any specific region. FRONTSPH was fitted to match the frontal brain regions and OCCISPH was fitted to the local curvature of the occipito-parietal regions. The origins of these models, which differ mainly in the anterior–posterior direction, are given in Table 1 in a head coordinate system, where the x-axis runs through points anterior to the ear canals (from left to right), the y-axis is perpendicular to the x-axis and runs through the nasion, and the z-axis is orthogonal to the xy-plane and points towards the top of the head.

To build a realistically shaped head model, one has to define the outline of the brain volume, which is typically done by defining the inner surface of the skull. For an even more accurate description of the conductor geometry of the whole head, the outer surfaces of the skull and the scalp must also be determined from anatomical head images. For the brain and scalp volumes, this can nowadays be done in a rather straightforward manner using 3D region growing algorithms. The segmentation of the skull layer is, however, more laborious as bone is not readily distinguishable in

Table 1
The head conductor models used in the simulations

Spherical conductor models							
Name	Origin						
BRAINSPH	$x = 1.0$, $y = 8.8$, $z = 41.6$ (mm)						
FRONTSPH	$x = 0.6$, $y = 21.1$, $z = 40.1$ (mm)						
OCCISPH	$x = 1.5$, $y = 0.7$, $z = 44.0$ (mm)						
Realistically shaped one-layer models							
Name	# of triangles	Side length (mm)					
1L6	4216	6					
1L10	1610	10					
1L14	830	14					
Realistically shaped 3-layer models							
	Brain compartment		Skull compartment		Scalp compartment		Total # of triangles
Name	# of triangles	Side length (mm)	# of triangles	Side length (mm)	# of triangles	Side length (mm)	
3L101010	1610	10	2434	10	2906	10	6950
3L101414	1610	10	1264	14	1538	14	4412
3L101818	1610	10	766	18	952	18	3328
3L121212	1120	12	1730	12	2044	12	4894
3L141014	830	14	2434	10	1538	14	4802
3L141410	830	14	1264	14	2906	10	5000
3L141414	830	14	1264	14	1538	14	3632
REFMODEL	2452	8	3772	8	4412	8	10636

REFMODEL was used in generation of the simulated magnetic fields. All the other models were used in the estimation of the active source areas. For the spherical models, the sphere origin is listed (in head coordinates, see text for details) and for the realistically shaped models, the number of triangles per compartment/model and the approximate triangle side length.

typical anatomical T_1-weighted MRIs and a lot of manual work might be required (Husberg, 2001).

When the different head compartments have been defined, a realistically shaped head model can be constructed using the boundary-element method (BEM; see e.g. Barnard et al., 1967; Brebbia et al., 1984; Hämäläinen and Sarvas, 1989), where the shape of each compartment is described using closed triangle meshes. The conductivity inside each compartment is assumed isotropic and homogeneous. The more triangles one uses in the mesh, the more accurately the model follows the true shape of the compartment and the more accurately the magnetic fields can be calculated. On the other hand, with the number of the triangles used, the size of the model and the amount of time required for the computations increase rapidly. Even though multi-layer models are nowadays feasible, typically only one-layer models (brain compartment) have been used in MEG. The contribution of the skull and scalp compartments to the accuracy of the model is considered relatively small due to the poor conductivity of the skull with respect to the brain tissue (Hämäläinen and Sarvas, 1989). The situation is, therefore, different from EEG where it is probably more important to model the skull as its presence smears the electric potentials measured on the scalp (Nunez, 1981).

The reference model in the present simulation study was a 3-layer realistically shaped BEM model that was as refined as possible (i.e. the total number of triangles in the model as high as possible). The limiting factor in the size of the model is the amount of computational time and memory needed to handle the model. For the reference model, illustrated in Fig. 1, the triangle meshes of all the compartments (brain, skull, and scalp) were created with triangle side length of approximately 8 mm. The conductivities of the different compartments were 0.3 S/m for the brain, 0.006 S/m for the skull, and 0.3 S/m for the scalp. The ratio of brain, skull, and scalp conductivities was thus 1:1/50:1. Traditionally, this ratio has been estimated to be in the order of 1:1/80:1 (Rush and Driscoll, 1968, 1969; Cohen and Cuffin, 1983), but more recent results suggest that it is closer to 1:1/15:1 (Foster and Schwan, 1989; Oostendorp et al., 2000). The ratio we used was between these two views, but we also tested the effect of the conductivity ratio on the source localization results in one part of the study by using the ratio 1:1/15:1 for the reference model and ratios 1:1/50:1 and 1:1/15:1 for the source localization (see Section 3).

In the localization of simulated brain activity, we used several one- and 3-layer realistically shaped BEM models with different triangle side lengths. The different realistically shaped models are described in Table 1. By varying the number of triangles in different head compartments, we tested the effect that different compartments have on the source estimation accuracy of the 3-layer model.

2.4. Noise

All MEG measurements contain noise from the environment, i.e. from nearby electric cables, electric devices, moving vehicles etc. Performing the MEG measurements in a magnetically shielded room diminishes the effects of these sources. Frequent noise patterns can also be excluded using a signal-space-projection (SSP; see e.g. Uusitalo and Ilmoniemi, 1997) method where the known noise fields are removed from the measured signals.

In addition to the noise from the environment, MEG measurements contain other signals that interfere with the field patterns of interest and, therefore, affect the localization of the current sources. These signals are generated by the subject and they consist of, for example, magnetic fields from other parts of the brain, magnetic fields created by eye movements and blinks and muscles such as the heart and the jaw, and possibly also magnetic fields created by magnetic objects in the subject's clothing. Because all these signals mask the magnetic fields that are created by the neural currents of interest, they can all be considered noise. The measurement device will also generate additional, typically spatially uncorrelated, noise.

The effect of magnetic fields not linked to the studied brain activity (i.e. not time-locked to the stimulus

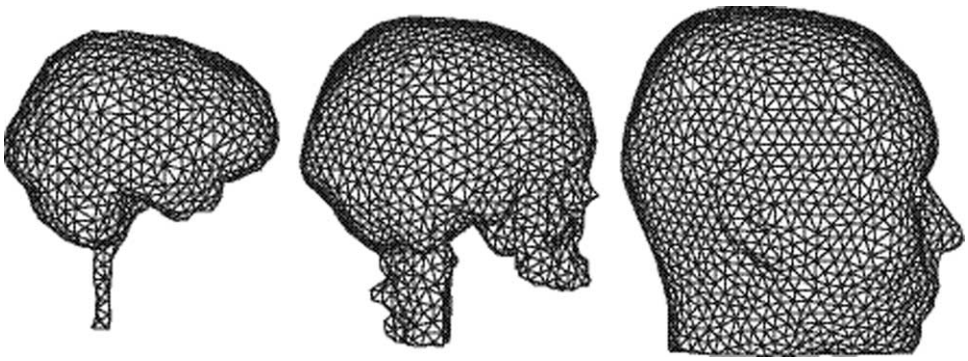

Fig. 1. Breakdown of the reference model used in the calculation of the simulated magnetic fields. From left to right, the triangle meshes describing the surface of the brain, skull, and scalp compartments.

presentation) can be reduced by averaging the brain responses with respect to stimulus or task onset. Some of the noise can also be removed by filtering the data.

In the present study, we added realistic noise to the magnetic fields generated by simulated current dipoles. The noise was calculated from real MEG data, which had been measured from a healthy human subject with the Vectorview™ magnetometer at the Helsinki University of Technology. We averaged the selected raw data file at randomly picked time points so that the resulting signal was not time-locked to the auditory stimuli that were used in the measurement. The number of averages was 100, which is typical also in real MEG measurements. The frequency content of the averaged noise signals was varied using low-pass filtering. Most of the results were calculated using noise low-pass filtered at 40 Hz, a typical pass-band in real data analysis. Some of the studies were repeated using noise that was low-pass filtered only at 100 Hz, thus including the always present and strong 50 Hz noise components from the main current.

To carry out the 9 repetitions at each studied source location, we formed 10 different noise signals from the same raw data file, averaged at 100 different, randomly picked time points. Nine of these signals were used to add the noise to the replications and the 10th noise signal was used as the baseline signal of the simulated data file.

The mean standard deviations of the averaged noise signals low-pass filtered at 100 Hz were 10.4 fT/cm for the gradiometers and 421 fT for the magnetometers when no SSP noise reduction was applied, and 6.8 fT/cm and 16.9 fT with SSP, respectively. The corresponding values for the noise signals low-pass filtered at 40 Hz were 4.7 fT/cm and 108 fT without SSP and 4.2 fT/cm and 11.5 fT with SSP, respectively. Because our noise signals were averaged from a real measurement file, they included the effect of noise from the environment, the measurement device, and the subject. To compare the effect of the conductor model geometry only on source localization, some of the simulations were performed without any noise.

In most of our simulations, the dipole strength was 30 nAm, which is a rather typical source strength in MEG recordings. Some of the simulations were repeated with 15 and 60 nAm dipoles, i.e. halving and doubling the original signal-to-noise ratio. For a certain filter setting, the noise level is the same for all brain areas. However, the absolute signal-to-noise ratio varies with source location as the signal strength depends on the distance between the source and the sensor grid and on the orientation of the source.

2.5. Source locations and orientations

We studied a total of 9599 different source locations. These locations formed an evenly spaced grid that occupied the whole brain volume with 5 mm spacing between the locations. All the locations were at least 2 mm away from the surface of the brain triangle mesh of the reference model. We placed current dipoles at these locations and calculated the simulated magnetic fields as seen by the 306-channel Vectorview™ magnetometer with only one dipole active at a time.

A radial current dipole placed inside a spherically symmetric conductor does not produce any magnetic field outside the conductor. The human brain is rather spherical and MEG is thus not equally sensitive to all current orientations. Therefore, if the orientation of a current dipole would be allowed to be totally random, not all different source locations would be treated equally, as sources that happen to be oriented optimally would create stronger fields and, therefore, better signal-to-noise ratio than unoptimally oriented sources. This would also affect the localization errors and mask the differences we would otherwise see with different source locations. We dealt with this problem in the following way. With realistically shaped models, we cannot define a strictly radial orientation. However, at any given location, we can find a current orientation that corresponds to the radial orientation in the sense that dipoles parallel to this orientation generate clearly weaker magnetic fields than dipoles parallel to the two remaining orthogonal components. This worst-case or quasi-radial direction can be found using singular value decomposition. At every source location, we used this method to define the quasi-radial direction and used only dipole orientations that were on a plane perpendicular to it. Within that plane, the source orientation was random. To further compensate for the possible effects of source orientation on the localization accuracy, we simulated 9 different source orientations (in the plane) at every source location, each with a slightly different noise field (see above).

The excluded 'quasi-radial' source orientations were determined with the realistically shaped reference model. The resulting dipoles were thus neither tangential with respect to the spherical models nor strictly 'quasi-tangential' with respect to the realistically shaped models used in the source estimation. The fact that 'quasi-radially' oriented currents are practically invisible in MEG is a feature of the method itself and does not depend on specific conductor models.

2.6. Calculation of magnetic fields and localization of current dipoles

The simulated magnetic fields were calculated in Matlab (The MathWorks Inc., Natick, MA, USA) utilizing functions written earlier in our laboratory. The calculations were performed using the linearly varying potential approximation for each triangle in the 3-layer reference model. Only one dipole was active at a time. The noise was added to the originally noiseless magnetic fields and the resulting fields were saved as a file readable by Xfit, the Neuromag source modeling software (Neuromag, 2001).

In the source localization program (Xfit), the head model was defined to be one of the spherical models, one-layer realistically shaped models, or 3-layer realistically shaped

models (the reference model was not used here). For dipole estimation, the source localization program makes first an initial guess of the source location by placing the dipole beneath the sensor showing the strongest signal. Thereafter, the nonlinear dipole fit algorithm attempts to find those dipole parameters that minimize the difference between the measured (here, simulated) magnetic field and the magnetic field generated by the dipole. With realistically shaped models, the program first computes the dipole with a spherical model and uses this dipole as the initial guess for the estimation procedure carried out with the realistically shaped model. The noise level for source modeling was estimated from the beginning of the file (baseline interval) where no current dipole was active. The effect of the constant noise sources known to be present in the measurement room was reduced by applying the SSP method. To test the effect of this noise reduction method, one computation was carried out without it.

Most of the procedures applied here replicated those normally used in dipole source localization with real MEG data. The only difference was that the source localization was done automatically with no interaction with the user. Therefore, all the MEG sensors (typically only the gradiometers, but in some cases only magnetometers or both gradiometers and magnetometers) were included in the source localization. In practice, the user often selects only a subset of sensors surrounding the apparent source area for the inverse calculation, which reduces the disturbance from other active brain areas. In our automatic localization procedure, this was neither technically practical nor necessary as only one dipole was active at a time.

After source modeling, the resulting dipole parameters (source location, amplitude, and orientation) were compared to the original ones and differences were calculated. The results were computed for all of the 9599 source locations but also for smaller source groups associated with certain brain areas and source depths (see Section 3). Occasionally, the source estimation can go clearly wrong giving meaningless results. In manual source estimation, results like these are easy to recognize and discard. In our automatic procedure, clear outliers (unusually large errors) were excluded from the calculations of the average results if the largest error differed from the mean result of the other replications in that source location by more than 5 times the standard deviation of the other replications.

3. Results

3.1. Localization accuracy in different parts of the brain with different head conductor models

The 3D topography of errors in estimating source location, amplitude, and orientation is displayed in Fig. 2 for the BRAINSPH model and in Fig. 3 for the 3L101010 model, in the presence of realistic noise low-pass filtered at 40 Hz. The original source amplitude was 30 nAm and localization was performed using gradiometers only and utilizing the SSP noise reduction. The two head conductor models gave remarkably similar results. Yet, in both models, the localization accuracy varied considerably with brain region. The source estimation was most successful around the vertex and in the frontoparietal and occipital areas. Errors in the temporal region were only slightly larger. Considerably worse results were obtained in the anterior frontal regions. Localization errors increased clearly with source depth, which is understandable as the signal-to-noise ratio decreases as the distance of the source from the sensors increases. The errors in all source parameters (location, amplitude, and orientation) were distributed in a very similar way.

The strong effect of brain region and the weak effect of conductor model on source estimation errors are evident in Fig. 4 and Table 2, which collect the data for the different conductor models. The differences between head conductor models were in most cases statistically highly significant (e.g. paired t test for the mean error in source location between BRAINSPH and 3L101010 gave $P = 0$ within the calculation accuracy). The proportion of highly accurate estimates (mean error smaller than 2 mm/2 nAm/4°) also increased from spherically symmetric to realistically shaped models. Yet, the absolute differences between models were so small that in many cases they are practically irrelevant. Some improvement can be gained especially in the anterior frontal regions by utilizing either a realistically shaped conductor model or a sphere matched to that region (FRONTSPH). However, a sphere matched to one specific region is often not a good choice for data analysis. If regions of interest include also other brain areas, such models tend to perform inferiorly outside the optimally matched brain area (e.g. FRONTSPH in the occipital region or the occipitally matched OCCISPH in the frontal regions).

As for the different 3-layer models, the most important factor for the accuracy, affecting especially the superficial sources, seemed to be the triangle size in the innermost brain compartment. The size of triangles in the other two compartments, the skull and the scalp, did not affect the results that much.

The errors in source amplitude (calculated for each source location as the mean absolute deviation from the original amplitude) suggest that for sources located relatively close to the brain surface (at depths of 2–15 mm), the realistically shaped models, in particular the 3-layer models, outperform the sphere models. However, for sources further away from the cortex, the situation is reversed, probably because the performance of realistically shaped models is not quite as stable as that of sphere models and occasionally results in considerable errors.

It should be noted that the original sources, simulated in the realistically shaped head model were not strictly tangential with respect to the spherical models. As spherical models see only the tangential component of the sources,

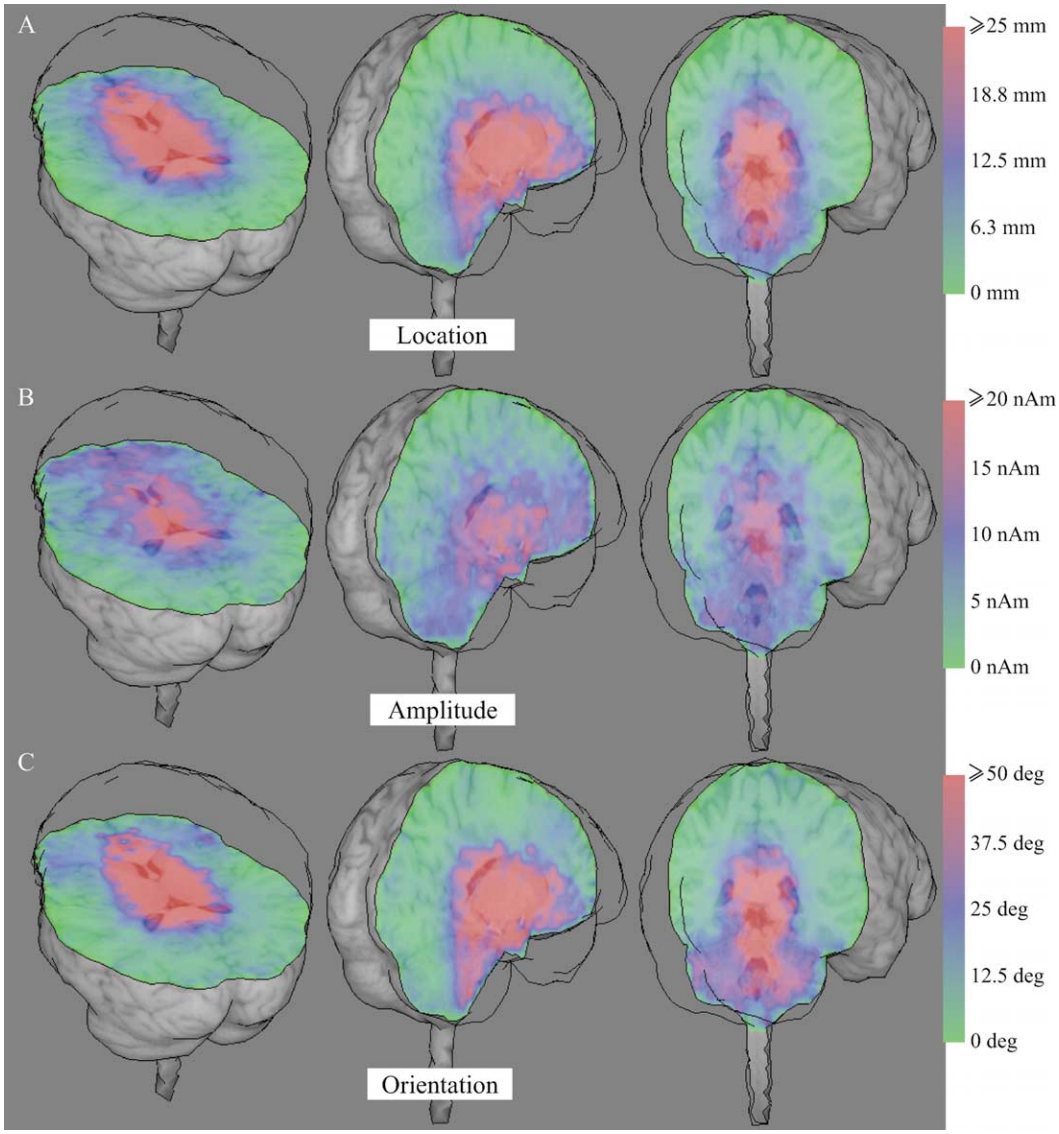

Fig. 2. The distribution of the source estimation errors using the BRAINSPH conductor model (30 nAm sources, noise low-pass filtered at 40 Hz, only gradiometers were included, and SSP noise projection was applied). Mean errors in (A) source location, (B) source amplitude, and (C) source orientation are color-coded and overlaid on anatomical MR images.

they cannot be expected to retrieve the exact amplitude or orientation even in noiseless cases. However, this is typically the case in real data analysis as well.

3.2. Effect of signal-to-noise ratio on the localization results

The results in Figs. 2–4 and Table 2 were calculated using noise that was low-pass filtered at 40 Hz. The effect of decreasing signal-to-noise ratio was tested with all 13 conductor models by re-calculating these data with noise that was low-pass filtered at 100 Hz. As expected, the higher noise level resulted in somewhat larger errors (Table 3) but the error distribution as well as the relative performance of the conductor models were very similar at both noise levels. On average, the source location errors increased by 3 mm. The effect of increased level of noise was very small (<1 mm) in areas where the localization accuracy was very good (occipital, frontoparietal, and temporal areas and around the vertex) but considerable (4–5 mm) in the more problematic areas (anterior frontal lobe and deep brain structures).

We manipulated the signal-to-noise ratio further using only conductor models BRAINSPH, 1L10, and 3L101818. We created simulated magnetic fields with original source amplitudes of 15, 30, and 60 nAm and used noise low-pass filtered both at 40 and 100 Hz. The localization errors as a function of source depth are presented in Fig. 5 where different line types correspond to the 3 different conductor models and different colors (red, black, and blue) to the 3 different source strengths. In addition, we estimated the current dipole parameters from magnetic fields that did not contain any noise at all (green curves; original source amplitude 30 nAm). The source depth is calculated as the distance from the surface of the brain

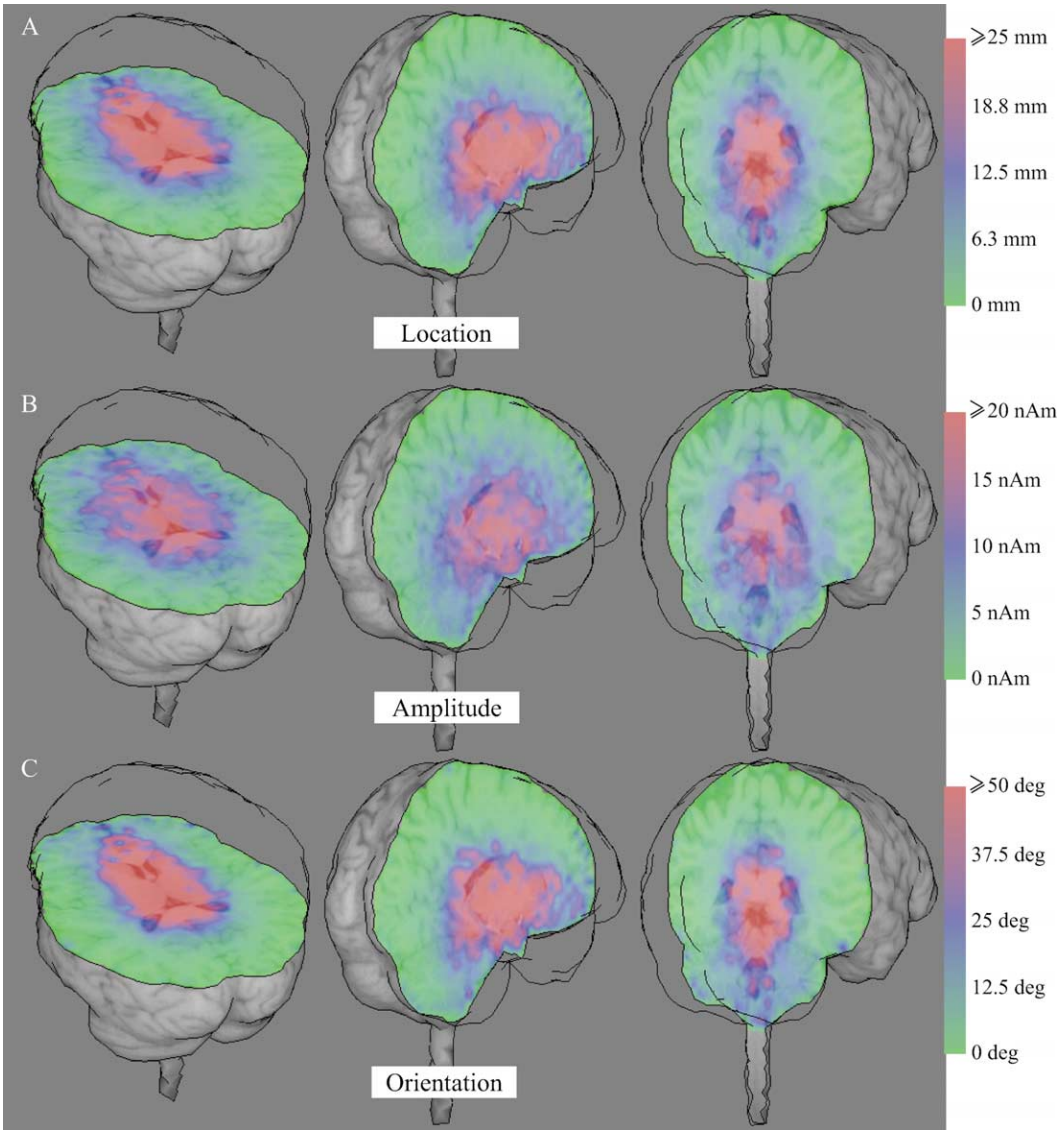

Fig. 3. The distribution of the source estimation errors using the 3L101010 conductor model (30 nAm sources, noise low-pass filtered at 40 Hz, only gradiometers were included, and SSP noise projection was applied). Mean errors in (A) source location, (B) source amplitude, and (C) source orientation are color-coded and overlaid on anatomical MR images.

triangle mesh of the reference model. Thus, all sources at small depths cannot be considered superficial, as a small portion of them is actually located at the base of the skull. Therefore, the results in Fig. 5 should be regarded as a comparison between different models and signal-to-noise ratios and an approximate description of the associated errors, rather than a detailed report of error magnitudes in different brain areas. Only gradiometers were used in these computations and the SSP noise reduction was applied to most conditions. The noiseless conditions (first column) were calculated without SSP noise reduction. The effect of SSP was also tested with noisy data (second and third columns) by calculating the results of the BRAINSPH model with and without SSP (dotted black and green curves).

The results show that the location, amplitude, and orientation estimates improved dramatically with increasing signal-to-noise ratio. At the lowest signal-to-noise ratio level (15 nAm sources; red curves in Fig. 5), deep sources as well as sources in the anterior frontal areas (not shown) produced large errors. However, even with relatively weak sources and noisy signals, the superficial sources could still be found quite reliably. In the noiseless condition (first column in Fig. 5), the 3-layer model 3L101818 differed clearly from the other two models, providing highly accurate estimates for all possible source locations. When noise was present, the choice of conductor model had little effect.

3.3. Effect of sensor type on the localization results

All previous results were computed using gradiometers only. The effect of sensor type was studied by repeating

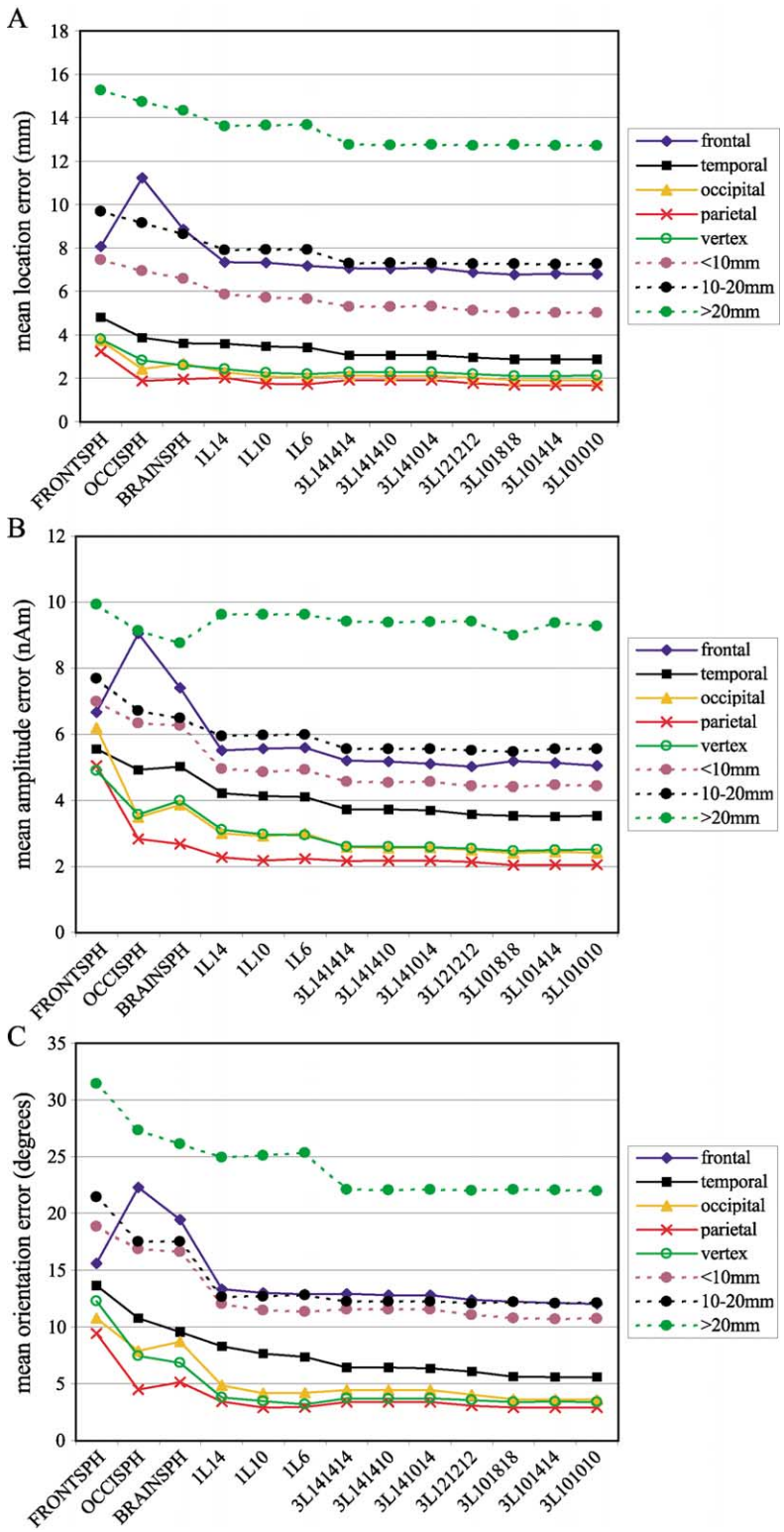

Fig. 4. The mean source estimation errors in (A) source location, (B) amplitude, and (C) orientation for all studied conductor models, grouped according to the original source location. The frontal, occipital, parietal, temporal, and vertex groups (colored solid curves) contained sources that were less than 15 mm away from the surface of the brain triangle mesh of the reference conductor model. The source locations were also divided into 3 groups based on the depth alone (<10 mm, 10–20 mm, and >20 mm; dashed curves). The original source amplitude was 30 nAm. The noise was low-pass filtered at 40 Hz and SSP noise reduction was applied during source estimation. Only gradiometers were used in source estimation.

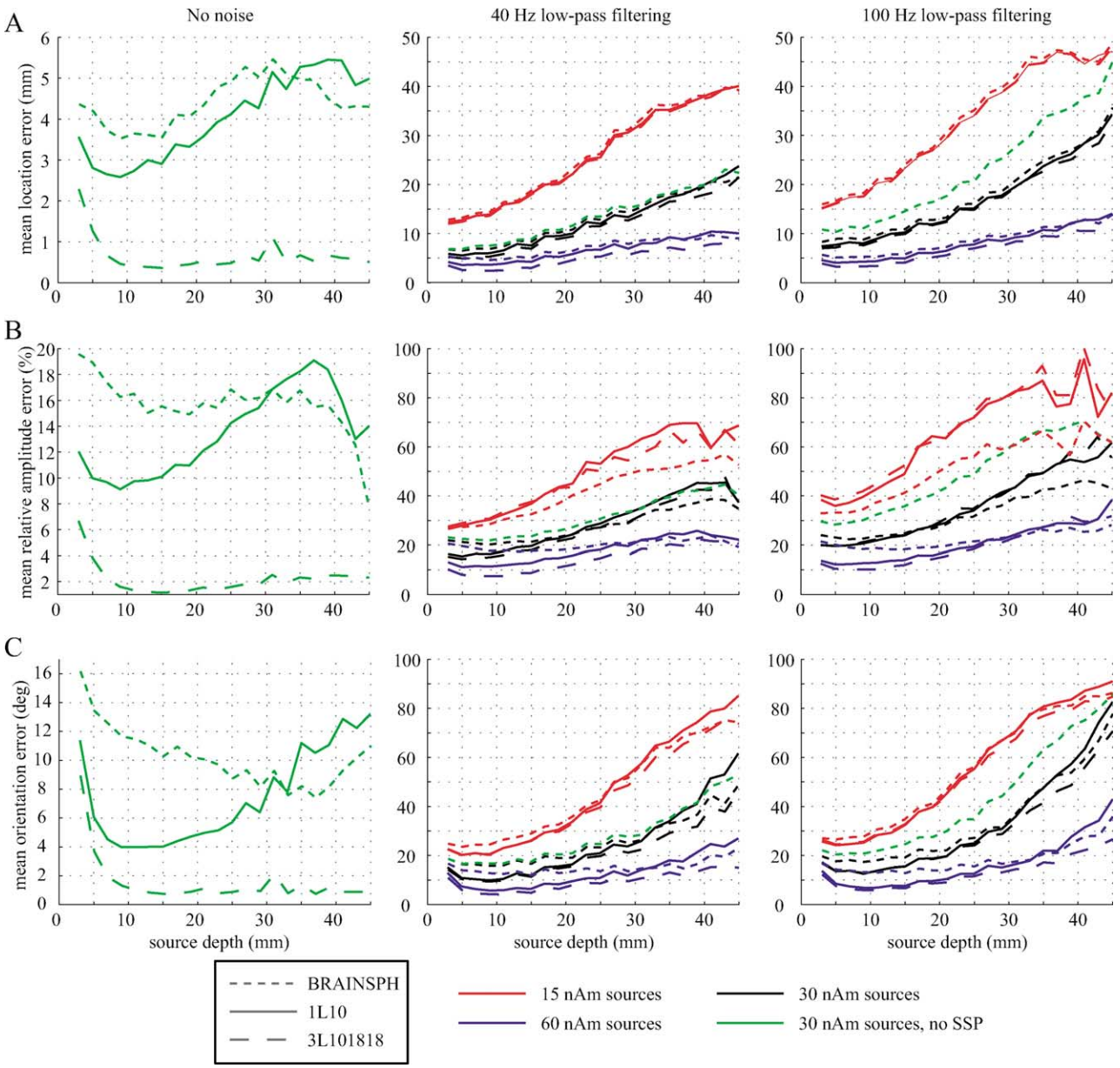

Fig. 5. The mean errors in source (A) location, (B) amplitude, and (C) orientation were calculated for BRAINSPH (dotted line), 1L10 (solid line), and 3L101818 (dashed line) models without any noise (first column), using noise low-pass filtered at 40 (middle column) and 100 Hz (third column). The source depth is measured as the distance from the surface of the brain triangle mesh of the reference model. The line color defines the original source strength (red = 15 nAm, black = 30 nAm, and blue 60 = nAm). Green color stands for the original source strength of 30 nAm and no SSP noise reduction in the source estimation (all 3 head models in the noiseless condition and only the BRAINSPH model in the noisy conditions). The amplitude errors are given relative to the original amplitude. Only gradiometers were used in source estimation.

some of the source estimates for the 102 magnetometers and the combination of magnetometers and gradiometers. The estimation errors are shown in Fig. 6 for noise low-pass filtered at 40 Hz.

In the studied case, the use of magnetometers did not improve the localization anywhere in the brain. However, as expected, the source depth had a weaker effect on the accuracy of the estimate when using magnetometers (gray curves in Fig. 6) than the more short-sighted gradiometers (thin black curves). This difference was particularly clear for the mean location errors.

3.4. Effect of the conductivity ratio of the brain, skull, and scalp compartments on the localization results

Due to different views (see Section 2) concerning the true conductivity ratios of the brain, skull, and scalp tissues, we tested how much the localization results are affected if the true conductivity ratio is 1:1/15:1, as suggested by Oostendorp et al. (2000), but the source analysis is performed using the ratio 1:1/50:1. To this end, we prepared a new reference model which differed from the one used in all our other simulations by the conductivity of the skull

Table 2
The source estimation errors with different conductor models (30 nAm sources, noise low-pass filtered at 40 Hz, magnetometers excluded, SSP noise reduction on)

	BRAINSPH	FRONTSPH	OCCISPH	1L6	1L10	1L14	3L101010	3L101414	3L101818	3L121212	3L141014	3L141410	3L141414
Errors in source location (mm)													
Mean ± SEM	9.6 ± 0.1	10.5 ± 0.1	10.0 ± 0.1	8.8 ± 0.1	8.8 ± 0.1	8.8 ± 0.1	8.1 ± 0.1	8.0 ± 0.1	8.1 ± 0.1	8.1 ± 0.1	8.2 ± 0.1	8.2 ± 0.1	8.2 ± 0.1
Median	5.5	6.4	5.9	5.0	5.0	5.0	4.4	4.4	4.4	4.4	4.5	4.5	4.5
% (<2 mm)	6.9	0.3	8.9	14.5	12.8	10.3	16.7	16.6	16.7	15.1	13.3	13.3	13.2
Errors in source amplitude (nAm)													
Mean ± SEM	7.08 ± 0.04	8.10 ± 0.04	7.29 ± 0.04	6.67 ± 0.05	6.65 ± 0.05	6.67 ± 0.05	6.24 ± 0.05	6.28 ± 0.05	6.13 ± 0.05	6.28 ± 0.05	6.32 ± 0.05	6.32 ± 0.05	6.33 ± 0.05
Median	6.1	7.2	6.3	5.3	5.3	5.3	4.5	4.5	4.5	4.6	4.6	4.6	4.6
% (<2 nAm)	3.4	1.2	3.4	7.5	7.5	6.5	11.6	11.5	11.6	10.9	10.1	10.0	10.0
Errors in source orientation (degrees)													
Mean ± SEM	19.7 ± 0.2	23.5 ± 0.2	20.2 ± 0.2	16.0 ± 0.2	15.9 ± 0.2	16.1 ± 0.2	14.5 ± 0.2	14.5 ± 0.2	14.6 ± 0.2	14.7 ± 0.2	14.9 ± 0.2	14.9 ± 0.2	14.9 ± 0.2
Median	11.4	15.2	13.5	8.1	8.1	8.3	6.5	6.5	6.6	6.7	7.0	6.9	7.0
% (<4°)	3.0	1.1	7.7	24.7	24.1	21.3	31.1	30.9	30.8	28.4	26.8	26.7	26.6

The mean (± standard error of mean, SEM) and median location, amplitude, and orientation errors are calculated from all source locations. In addition, the percentage of very good localization results (mean error smaller than 2 mm/2 nAm/4°) are given for all conductor models.

Table 3
The source estimation errors with different conductor models (30 nAm sources, noise low-pass filtered at 100 Hz, magnetometers excluded, SSP noise reduction on)

	BRAINSPH	FRONTSPH	OCCISPH	1L6	1L10	1L14	3L101010	3L101414	3L101818	3L121212	3L141014	3L141410	3L141414
Errors in source location (mm)													
Mean ± SEM	12.6 ± 0.2	13.5 ± 0.1	13.1 ± 0.2	11.7 ± 0.1	11.7 ± 0.1	11.8 ± 0.1	11.4 ± 0.1	11.4 ± 0.1	11.4 ± 0.1	11.4 ± 0.1	11.5 ± 0.1	11.5 ± 0.1	11.5 ± 0.1
Median	6.7	7.4	7.0	6.2	6.2	6.2	5.9	5.9	5.9	6.0	6.0	6.0	6.0
% (<2 mm)	4.1	0.3	5.6	8.5	7.6	5.6	8.7	8.6	8.7	7.6	6.5	6.4	6.4
Errors in source amplitude (nAm)													
Mean ± SEM	8.15 ± 0.05	8.85 ± 0.05	8.33 ± 0.05	8.15 ± 0.06	8.13 ± 0.06	8.15 ± 0.06	8.51 ± 0.07	8.58 ± 0.07	8.25 ± 0.07	8.65 ± 0.08	8.58 ± 0.07	8.48 ± 0.07	8.56 ± 0.07
Median	7.1	7.8	7.3	6.5	6.5	6.4	6.2	6.2	6.1	6.2	6.2	6.2	6.2
% (<2 nAm)	1.7	0.8	1.9	4.3	4.5	3.6	5.8	5.7	5.7	4.9	4.6	4.5	4.6
Errors in source orientation (degrees)													
Mean ± SEM	23.5 ± 0.3	27.2 ± 0.3	24.0 ± 0.2	20.4 ± 0.2	20.5 ± 0.2	20.6 ± 0.2	19.7 ± 0.2	19.7 ± 0.2	19.7 ± 0.2	19.9 ± 0.2	20.0 ± 0.2	20.0 ± 0.2	20.0 ± 0.2
Median	13.0	16.5	15.1	10.1	10.2	10.3	8.8	8.8	8.8	9.0	9.2	9.2	9.2
% (<4°)	2.4	0.7	5.8	17.9	17.3	13.9	19.8	19.8	19.9	18.0	16.0	16.1	16.0

The mean (± SEM) and median location, amplitude, and orientation errors are calculated from all source locations. In addition, the percentage of very good localization results (mean error smaller than 2 mm/2 nAm/4°) are given for all conductor models.

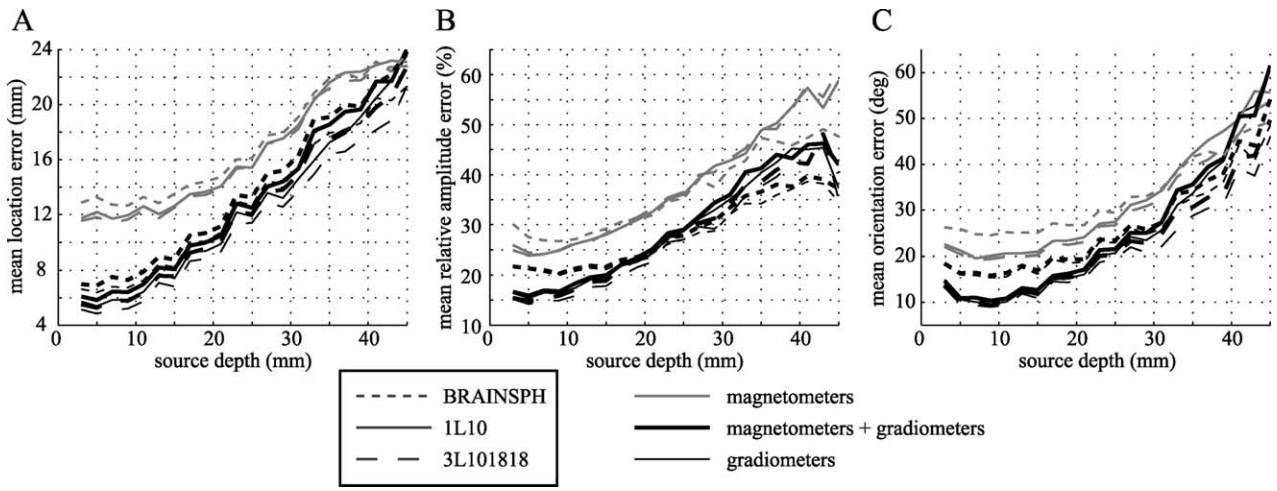

Fig. 6. The mean errors in source (A) location, (B) amplitude, and (C) orientation were calculated for BRAINSPH (dotted line), 1L10 (solid line), and 3L101818 (dashed line) models using only magnetometers (gray line), gradiometers (thin black line), or the combination of both (thick black line). The amplitude errors are given relative to the original amplitude (30 nAm). The noise was low-pass filtered at 40 Hz and SSP noise reduction was applied during source estimation.

which was increased to 0.02 S/m, rendering the desired ratio of 1:1/15:1. Using this reference model, we recalculated the magnetic field patterns generated by 30 nAm sources, with noise low-pass filtered at 40 Hz. Because the skull compartment was of special interest, we replaced the 3L101818 model used above with the computationally heavy 3L101010 model. The source parameters were thus estimated using the models BRAINSPH, 1L10, and 3L101010 (with conductivity ratio 1:1/50:1) but also with a new model 3L101010B, which had the same conductivity ratio (1:1/15:1) as the reference model used here. The localization errors are shown in Fig. 7. The gray curves depict the source estimation errors for BRAINSPH, 1L10, and 3L101010 models when the magnetic fields had been simulated using the new reference model (1:1/15:1 conductivity ratio). To aid comparison, black lines indicate the errors when the reference model was the standard one (1:1/50:1 conductivity ratio).

The results (Fig. 7) show that using the correct value (model 3L101010B; dark gray curve) instead of underestimating the conductivity of the skull improved the source estimation accuracy in deep source areas, especially in the estimation of the source amplitude. However, the exact value of the conductivity of the skull, at least in the studied range, did not seem to be critical for the success of the source estimation.

4. Discussion

To obtain the topography of MEG source estimation errors in the entire brain volume, in the presence of realistic noise, we computed more than 4.5 million equivalent current dipole solutions using 13 different head conductor models. The different head conductor models performed almost equally well in most parts of the brain. The spherical model BRAINSPH optimally describing the entire cranial volume gave localization errors that were only slightly larger than the results obtained with the computationally much heavier realistically shaped models. The small advantage of realistically shaped BEM models decreased with decreasing signal-to-noise ratio. When the level of noise was increased or the original source strength decreased, the mean localization errors increased and the differences between different conductor models became less obvious, in agreement with the EEG findings of Cuffin (1996) and Vanrumste et al. (2002). The performance of a sphere model can be improved by using a model specifically fitted for the area of interest. This, however, decreases the performance of the model in brain regions far away from the area of interest.

Our results show that even though small improvements can be gained using more complex conductor models, the conventional sphere model is adequate for many practical measurement situations, such as the analysis of signals from auditory, visual, motor, and somatosensory cortices. In these areas, the active source areas can often be localized with 2–4 mm accuracy, in accordance with previous findings (Menninghaus et al., 1994; Tomita et al., 1996; Leahy et al., 1998; Crouzeix et al., 1999), leaving only little room for improvements from the use of more advanced conductor models. The mean localization errors increased a few millimetres for the inferior temporal regions. In the anterior frontal lobe and deep brain structures, which are the two most problematic areas for source localization, the mean errors in source location often exceeded 1 cm and in several cases even 2 cm. The estimation of the source amplitude and orientation was most flawed in these same areas. It is important to note that the large errors in source estimation in these areas are mostly due to the reduced signal-to-noise

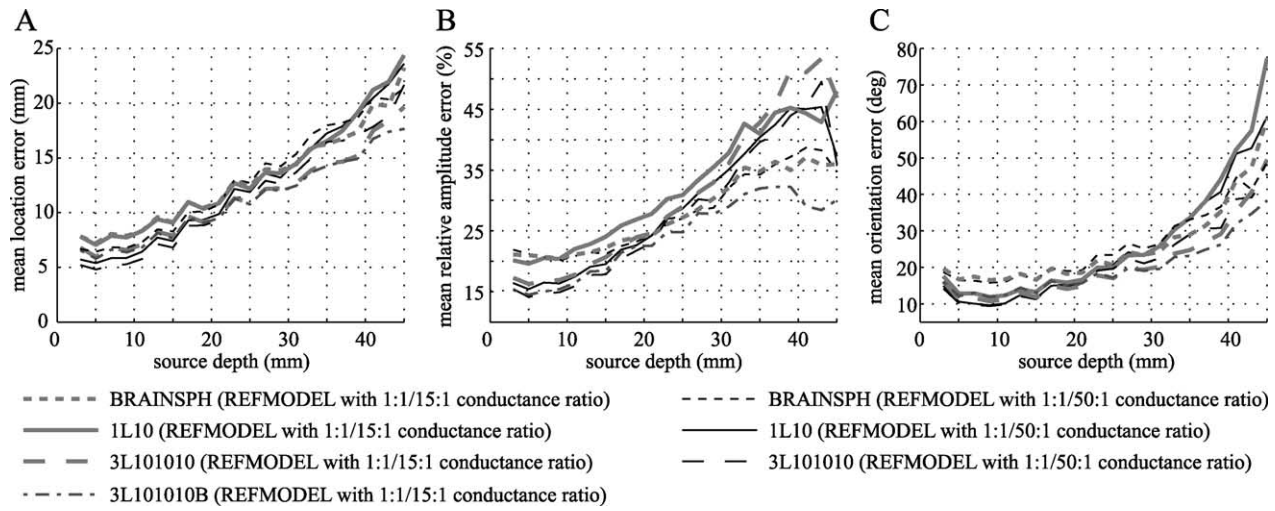

Fig. 7. The mean source estimation errors in source (A) location, (B) amplitude, and (C) orientation were calculated for BRAINSPH, 1L10, and 3L101010 models from signals that were simulated with the standard reference model (black lines; 1:1/50:1 conductivity ratio) and with a new reference model (gray lines; 1:1/15:1 conductivity ratio). The 3L101010B model (dark gray line) had the same conductivity ratio as the new reference model and it was only used with data from the new reference model. The amplitude errors are given relative to the original amplitude (30 nAm). The noise was low-pass filtered at 40 Hz and SSP noise reduction was applied during source estimation. Only gradiometers were used in source estimation.

ratio as similar behavior was seen with all conductor models tested here. However, these are still the areas where one might benefit most from the use of realistically shaped conductor models.

The use of a one-layer BEM model instead of a spherical model, especially in the anterior frontal lobe, can lead to improvements of about 2 mm in the accuracy of source location. The use of a 3-layer BEM model can improve the accuracy even further. The noiseless simulations carried out here and in our previous study (Husberg, 2001) showed that with the 3-layer BEM models, the accuracy of source estimation was approximately the same everywhere in the brain volume. Obviously, this spatial homogeneity may be partly due to the fact that our reference model was also a 3-layer BEM model (although more refined than the ones used in source estimation), which, to some degree, may favor the results obtained with other 3-layer models. All the same, the use of realistically shaped conductor models tends to improve the accuracy of the estimation of source parameters, including not only source location but also, and perhaps even more importantly, source strength and orientation. Therefore, the use of refined realistically shaped conductor models may certainly be helpful. However, it is apparently not vital, as the dominant source of errors seems to be the presence of noise.

If one prefers to use a realistically shaped BEM model, a one-layer model with a large number of triangles (e.g. 1L10) works well. To create as good a conductor model as possible, the best candidate is a multi-layer model that takes into account the conductivity of the different tissues of the head. The most important factor here seems to be the modeling of the innermost layer, i.e. the brain compartment. While keeping the total complexity of the model fixed, the brain compartment should be described with highest accuracy (smallest triangles) whereas the skull and scalp layers can be modeled less accurately. This solution is in agreement with our earlier results in the noiseless case (Husberg, 2001) and the EEG-based simulations of Fuchs et al. (2001). The functionality of such a brain model can be further increased by using sophisticated techniques, such as the virtual refinement of triangles (Fuchs et al., 1998a), not tested here.

The obvious reason for the small differences seen in the results between different conductor models is the realistic noise that was added to the simulated magnetic fields. This was also shown by the tests where the signal-to-noise ratio was varied. Clear differences between the 3-layer head model and the other models were obtained only in the noiseless situation, with the magnitude of the errors in that particular condition agreeing with previous reports (Crouzeix et al., 1999; Husberg, 2001). Previous studies have shown that for a given sensor array and dipole location, the mean localization errors are proportional to the inverse of the signal-to-noise ratio (Mosher et al., 1993; Fuchs et al., 1998b). A similar behavior was also visible in the results presented here (Fig. 5). Accordingly, the most efficient ways to increase the localization accuracy are the enhancement of the signal strength, e.g. by optimizing the stimulus presentation parameters, and the reduction of noise by increasing the number of averages collected, screening the external noise sources as well as possible, and applying noise reduction techniques such as filtering and the SSP method utilized in the present study.

The test conducted here did not show any general improvement by using magnetometers in addition to gradiometers—not even for deep source areas. Gradiometers outperformed magnetometers, most probably owing to their smaller noise sensitivity. The interfering

brain signals originating mostly in the cortex may have nullified the theoretical advantage magnetometers have in seeing activity from deep brain structures. If the effect of these cortical signals is eliminated e.g. by high-pass filtering, magnetometers will yield better results (Lauri Parkkonen, personal communication; results to be published).

5. Limitations of the results: possible improvements for future studies

Our simulations did not specifically deal with the situation where two or even more strong source areas are active simultaneously, which is often the case in real data analysis. Several equally active source areas make the data analysis harder and the possibility for errors increases, which is at least partly demonstrated here with deep source areas that evoked only weak signals compared with the noise level. In practice, these situations can be dealt with by identifying a time point where the interference from other sources is minimal and by taking into account only those sensors that cover the source area of interest, thereby maximizing the signal-to-noise ratio.

In reality, the neural currents flowing in the brain are not point-like objects (current dipoles) but they have a certain spatial extent. Nevertheless, in many cases, the activated area is relatively small compared with the distance to the sensors and, in this case, a point-like current dipole is a reasonable approximation. However, the shape and extent of the source area would be an important additional variable in simulating real brain activations.

The reference model is never perfect. With increasing computational power, the BEM model can be further refined. The results in the noiseless case, where errors for the most superficial source locations (at depths of 2–4 mm) were somewhat larger than for slightly deeper (5–10 mm) sources, suggest that the reference model did not perform optimally for sources that were very close to the innermost triangle mesh. This situation could probably be improved by using a mesh with smaller triangles. Other approaches for modeling the conductivity profile, such as the finite-element method that can represent local tissue conductivity changes (see e.g. Haueisen et al., 1997, 2000), could also be tested.

It should also be noted that the results presented here are mean errors. For single source areas, the errors can be clearly larger or smaller. The errors presented here include the effect of noise and conductor model. As mentioned in Section 1, the source localization accuracy depends also on other factors, which may increase the total error. Many of those factors, such as head movements during the measurement (Uutela et al., 2001), can be controlled and accounted for.

Acknowledgements

We wish to thank Matti Hämäläinen and Kimmo Uutela for many of the programs and functions used in this study as well as for help and comments in preparation of this study and Lauri Parkkonen for comments on the manuscript. This work was supported by the Academy of Finland (grant nos. 49900 and 44879, Finnish Centre of Excellence Programme 2000–2005), the Ministry of Education of Finland, European Union FP5 programme (QLK6-CT-1999-02140), and the Foundation of Vilho, Yrjö, and Kalle Väisälä (Finnish Academy of Science and Letters).

References

Balish M, Sato S, Connaughton P, Kufta C. Localization of implanted dipoles by magnetoencephalography. Neurology 1991;41:1072–6.

Barnard AC, Duck IM, Lynn MS, Timlake WP. The application of electromagnetic theory to electrocardiology. II. Numerical solution of the integral equations. Biophys J 1967;7:463–91.

Brebbia CA, Telles JCF, Wrobel LC. Boundary element techniques. Berlin: Springer Verlag; 1984.

Cohen D, Cuffin BN. Demonstration of useful differences between magnetoencephalogram and electroencephalogram. Electroenceph clin Neurophysiol 1983;56:38–51.

Crouzeix A, Yvert B, Bertrand O, Pernier J. An evaluation of dipole reconstruction accuracy with spherical and realistic head models in MEG. Clin Neurophysiol 1999;110:2176–88.

Cuffin BN. EEG localization accuracy improvements using realistically shaped head models. IEEE Trans Biomed Eng 1996;43:299–303.

Dale AM, Liu AK, Fischl BR, Buckner RL, Belliveau JW, Lewine JD, et al. Dynamic statistical parametric mapping: combining fMRI and MEG for high-resolution imaging of cortical activity. Neuron 2000;26:55–67.

Foster KR, Schwan HP. Dielectric properties of tissues and biological materials: a critical review. Crit Rev Biomed Eng 1989;17:25–104.

Fuchs M, Drenckhahn R, Wischmann HA, Wagner M. An improved boundary element method for realistic volume-conductor modeling. IEEE Trans Biomed Eng 1998a;45:980–97.

Fuchs M, Wagner M, Wischmann HA, Kohler T, Theissen A, Drenckhahn R, et al. Improving source reconstructions by combining bioelectric and biomagnetic data. Electroenceph clin Neurophysiol 1998b;107:93–111.

Fuchs M, Wagner M, Kastner J. Boundary element method volume conductor models for EEG source reconstruction. Clin Neurophysiol 2001;112:1400–7.

Godey B, Schwartz D, de Graaf JB, Chauvel P, Liegeois-Chauvel C. Neuromagnetic source localization of auditory evoked fields and intracerebral evoked potentials: a comparison of data in the same patients. Clin Neurophysiol 2001;112:1850–9.

Gross J, Kujala J, Hämäläinen M, Timmermann L, Schnitzler A, Salmelin R. Dynamic imaging of coherent sources: studying neural interactions in the human brain. Proc Natl Acad Sci USA 2001;98:694–9.

Hämäläinen M, Hari R, Ilmoniemi RJ, Knuutila J, Lounasmaa OV. Magnetoencephalography—theory, instrumentation, and applications to noninvasive studies of the working human brain. Rev Mod Phys 1993;65:413–97.

Hämäläinen MS, Sarvas J. Realistic conductivity geometry model of the human head for interpretation of neuromagnetic data. IEEE Trans Biomed Eng 1989;36:165–71.

Haueisen J, Ramon C, Eiselt M, Brauer H, Nowak H. Influence of tissue resistivities on neuromagnetic fields and electric potentials studied with

a finite element model of the head. IEEE Trans Biomed Eng 1997;44: 727–35.

Haueisen J, Ramon C, Brauer H, Nowak H. The influence of local tissue conductivity changes on the magnetoencephalogram and the electroencephalogram. Biomed Tech (Berl) 2000;45:211–4.

Husberg M. The use of a three-layer boundary-element model in localization of brain activity. Special assignment Tfy-99.298, Department of Engineering Physics and Mathematics, Helsinki University of Technology (Finland) 2001.

Leahy RM, Mosher JC, Spencer ME, Huang MX, Lewine JD. A study of dipole localization accuracy for MEG and EEG using a human skull phantom. Electroenceph clin Neurophysiol 1998;107:159–73.

Mäkelä JP, Kirveskari E, Seppä M, Hämäläinen M, Forss N, Avikainen S, et al. Three-dimensional integration of brain anatomy and function to facilitate intraoperative navigation around the sensorimotor strip. Hum Brain Mapp 2001;12:180–92.

Menninghaus E, Lütkenhöner B, Gonzalez SL. Localization of a dipolar source in a skull phantom: realistic versus spherical model. IEEE Trans Biomed Eng 1994;41:986–9.

Mosher JC, Leahy RM. Source localization using recursively applied and projected (RAP) MUSIC. IEEE Trans Signal Process 1999;47:332–40.

Mosher JC, Spencer ME, Leahy RM, Lewis PS. Error bounds for EEG and MEG dipole source localization. Electroenceph clin Neurophysiol 1993;86:303–21.

Neuromag. Source Modelling Software User's Guide, Software version 5.2.4, 2001

Nunez PL. Electric fields of the brain. New York, NY: Oxford University Press; 1981.

Oostendorp TF, Delbeke J, Stegeman DF. The conductivity of the human skull: results of in vivo and in vitro measurements. IEEE Trans Biomed Eng 2000;47:1487–92.

Rose DF, Sato S, Ducla-Soares E, Kufta CV. Magnetoencephalographic localization of subdural dipoles in a patient with temporal lobe epilepsy. Epilepsia 1991;32:635–41.

Rush S, Driscoll DA. Current distribution in the brain from surface electrodes. Anesth Analg 1968;47:717–23.

Rush S, Driscoll DA. EEG electrode sensitivity—an application of reciprocity. IEEE Trans Biomed Eng 1969;16:15–22.

Sekihara K, Nagarajan SS, Poeppel D, Marantz A, Miyashita Y. Reconstructing spatio-temporal activities of neural sources using an MEG vector beamformer technique. IEEE Trans Biomed Eng 2001;48: 760–71.

Tomita S, Kajihara S, Kondo Y, Yoshida Y, Shibata K, Kado H. Influence of head model in biomagnetic source localization. Brain Topogr 1996; 8:337–40.

Uusitalo MA, Ilmoniemi RJ. Signal-space projection method for separating MEG or EEG into components. Med Biol Eng Comput 1997;35: 135–40.

Uutela K, Hämäläinen M, Somersalo E. Visualization of magnetoencephalographic data using minimum current estimates. Neuroimage 1999;10:173–80.

Uutela K, Taulu S, Hämäläinen M. Detecting and correcting for head movements in neuromagnetic measurements. Neuroimage 2001;14: 1424–31.

Vanrumste B, Van Hoey G, Van de Walle R, D'Have MR, Lemahieu IA, Boon PA. Comparison of performance of spherical and realistic head models in dipole localization from noisy EEG. Med Eng Phys 2002;24: 403–18.

Yvert B, Bertrand O, Thevenet M, Echallier JF, Pernier J. A systematic evaluation of the spherical model accuracy in EEG dipole localization. Electroenceph clin Neurophysiol 1997;102:452–9.